CELL SEGMENTATION AND TRACKING IN PHASE CONTRAST IMAGES USING GRAPH CUT WITH ASYMMETRIC BOUNDARY COSTS

Robert Bensch[1,2] *Olaf Ronneberger*[1,2]

[1] Image Analysis Group, Computer Science Department, University of Freiburg, Germany
[2]BIOSS Centre for Biological Signalling Studies, University of Freiburg, Germany

ABSTRACT

We propose a new robust, effective, and surprisingly simple approach for the segmentation of cells in phase contrast microscopy images. The key feature of our algorithm is that it strongly favors dark-to-bright transitions at the boundaries of the (arbitrarily shaped) segmentation mask. The segmentation mask can be effectively found by a fast min-cut approach. The small but essential difference to standard min-cut based approaches is that our graph contains directed edges with asymmetric edge weights. Combined with a simple region propagation our approach yields better segmentation results on the ISBI Cell Tracking Challenge 2014 dataset than the top ranked methods. We provide an easy-to-use open-source implementation for ImageJ/Fiji and Matlab on our homepage.

Index Terms— cell segmentation, cell tracking, phase contrast microscopy, graph-cut, min-cut, asymmetric boundary costs

1. INTRODUCTION

Since its invention around 75 years ago, phase contrast microscopy [1] has become the premier choice to visualize thin transparent regions in living cells (Fig. 1a). The advantageous high contrast at the cell borders comes with several artifacts, like shade-off and halo patterns [2], which complicate an automated segmentation. The shade-off effect increases the inner cell intensity to the same level as the surrounding medium, which hamper the application of simple region-based approaches. Additionally both effects can introduce strong edges inside and outside of the cell, which then guide standard edge-based algorithms (see Fig. 1b) to the wrong positions.

In this paper we propose a principled solution that makes use of the fact that the true cell borders in positive phase contrast microscopy always appear as a dark-to-bright transition in outwards direction. I.e. all borders with an inverse transition (bright-to-dark) are definitely not the sought cell borders. For simple morphologies, like roundish or star-shaped cells, the wrong borders could be easily suppressed in a pre-processing step. However, for more complicated morphologies (see Fig. 5) the outwards-direction depends on the local border-normal of the resulting segmentation mask, which is not available in advance. We solve this problem by minimizing an energy functional that searches for a segmentation mask and simultaneously favors dark-to-bright transitions at its boundary. Discretization of this functional yields a combinatorial optimization problem that can be solved efficiently by a min-cut approach (Fig. 1c). The important difference to the usual application of min-cuts in image segmentation is the use of a graph with directed edges and asymmetric edge costs.

We show that this approach results in a large improvement regarding quality and robustness in phase contrast images. At the same time, it inherits all the advantageous properties of min-cut segmentation, like global optimality, simultaneous optimization of region and boundary terms, and computational efficiency.

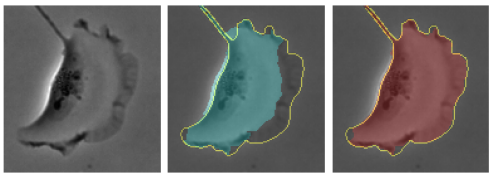

(a) (b) (c)

Fig. 1: Cell segmentation for phase contrast images. **(a)** Raw image. **(b)** Segmentation result with traditional graph cut (cyan), and ground truth contour (yellow). **(c)** Segmentation result with the proposed method (red).

In combination with a simple segmentation propagation our approach yields better segmentation results on the ISBI Cell Tracking Challenge dataset than the top ranked methods (evaluated on the *challenge* dataset). Furthermore, it is less complex and has fewer tuning parameters than the top ranked method [3].

We will provide the Matlab source code and a ready-to-use ImageJ/Fiji plugin upon publication at http://lmb.informatik.uni-freiburg.de/resources/opensource/.

1.1. Related work

Cell segmentation in phase contrast images has recently been extensively studied by the Kanade group (e.g. see [4]). They propose a two step approach by first reconstructing the absolute phase image and then applying basic threshold techniques. This technique works only for completely transparent samples. It fails if the sample contains light absorbing structures, because absorption induced intensity changes and phase-based intensity changes are indistinguishable in standard phase-contrast or DIC microscopic images. Ambühl et al. [5] propose a series of morphological image processing steps combined with level set approaches. They propose to overcome the problem of the strong halo edges by changing the image during the evolution of the level sets. They apply a morphological top-hat filter to temporally hide these edges until the contour has passed by. The approach by Magnusson et al. [3] is currently the top ranked method on the ISBI Cell Tracking Challenge dataset [6]. It mainly relies on a strong tracking approach using the Viterbi algorithm. To increase the performance for the ISBI challenge, they applied a segmentation algorithm based on bandpass filtering, thresholding and watershed transform, which requires several parameters to be adjusted.

The usage of asymmetric boundary costs in the min-cut segmentation was already proposed by Boykov in his original graph-cut segmentation paper [7], but never found its way to the phase contrast microscopy.

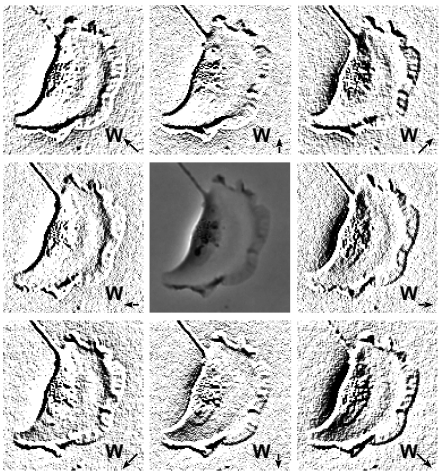

Fig. 2: Asymmetric boundary costs promote low costs at characteristic dark-bright intensity transitions at cells boundaries in phase contrast microscopy. Boundary costs at each pixel are shown in separate maps for each direction in an 8-connected pixel neighborhood (arrows indicate direction). Costs range from zero to one (black to white). The phase contrast image is shown in the middle.

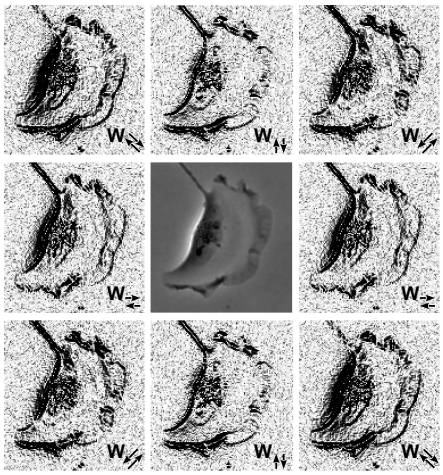

Fig. 3: Symmetric boundary costs, in contrast to asymmetric costs (Fig. 2), also yield low costs at irrelevant boundaries at bright-dark intensity transitions. Note that the pairs of opposed boundary maps are redundant in the case of symmetric costs.

2. METHODS

2.1. Cell segmentation

Phase contrast microscopy allows to visualize transparent objects. It turns the invisible phase shifts of the light waves originating from the object into visible intensity changes by using interference with the 90^o phase shifted illumination wave. Ideally this would result in an intensity decrease proportional to the object thickness. In reality other effects induce additional shade-off and halo patterns [2], such that the intensity drop is only reliably found at the object borders to the surrounding medium.

We set up a segmentation energy functional for a mask $M : \Omega \to \{0, 1\}$ with $\Omega \subset \mathbb{R}^2$ and the given image $I : \Omega \to \mathbb{R}$. The functional contains a data cost $C_{\text{obj}} : \mathbb{R} \to \mathbb{R}$ that depends on the intensity, and an edge cost $C_{\text{edge}} : \mathbb{R} \to \mathbb{R}$ that depends on the intensity gradient at the mask border in outwards direction

$$E(M) = \lambda \int_\Omega M(\mathbf{x}) \cdot C_{\text{obj}}(I(\mathbf{x}))d\mathbf{x} + \int_\Omega C_{\text{edge}} \left(\left\langle \nabla M(\mathbf{x}), -\nabla I(\mathbf{x}) \right\rangle \right) d\mathbf{x}, \quad (1)$$

where we define ∇M to be a unit normal vector on the mask boundary and $\mathbf{0}$ elsewhere. The data cost for a gray value v is derived from the foreground intensity histogram $P(v|\mathcal{O})$ and background intensity histogram $P(v|\mathcal{B})$ from training regions. We define it as $C_{\text{obj}}(v) = 1 - P(v|\mathcal{O})/(P(v|\mathcal{O}) + P(v|\mathcal{B}))$. The edge cost for the intensity derivative d is computed as

$$C_{\text{edge}}(d) = \begin{cases} \exp\left(-\frac{d^2}{2\sigma^2}\right) & \text{if } d > 0 \\ 1 & \text{else.} \end{cases} \quad (2)$$

I.e., the edge term in the energy functional favors dark-to-bright transitions at the mask borders.

To optimize this energy, we discretize the edge term into 8 directions and solve it by a min-cut as described in [7]. Compared to the "standard" min-cut segmentation approach, our approach results in a directed graph with asymmetric edge weights. In contrast, when using $\exp(-d^2/2\sigma^2)$ for both cases in Equ. 2, an undirected graph with symmetric edge weights is obtained.

Figs. 2 and 3 illustrate the benefit of using asymmetric costs over symmetric costs at an example. Asymmetric costs allow to favor low boundary costs at characteristic dark-bright intensity transitions at cell boundaries in phase contrast images (Fig. 2). Symmetric costs however yield non-specific boundary costs, since also irrelevant bright-dark transitions receive low costs (Fig. 3).

2.2. Cell tracking

Segmentation propagation Each frame is segmented using min-cut, which yields a binary segmentation mask. To promote temporal consistency, we propagate segmentation information from frame t to frame $t + 1$ in two fashions:

Foreground propagation: The eroded mask is set as hard foreground constraint for the min-cut segmentation in the next frame. This adds robustness to the region term in case of insufficient foreground evidence. The size of erosion must be chosen at least as large as the expected motion of object boundary pixels between frames.

Non-merging constraint: If it can be assumed that cells do not merge, it is reasonable to prevent separate objects from merging in the next frame. We achieve this by computing a distance transform on the segmentation mask and applying watershed transform seeded at the object locations. The boundaries of the herewith computed "support regions" of each object are set as hard background constraint.

For tracking, each segmented object is assigned a unique label that is propagated across the frames.

3. EXPERIMENTS

3.1. Dataset

We evaluated our method on challenging phase contrast microscopy videos of moving cells published by the Second ISBI Cell Tracking Challenge [6], [8]. We used the training dataset PhC-C2DH-U373 (provided by Dr. Sanjay Kumar from UC Berkeley). It contains two 2D sequences (115 frames each) of Glioblastoma-astrocytoma U373 cells on a polyacrylimide substrate. Cell segmentation and tracking ground truth is included, along with evaluation tools. Segmentation masks are available only for a subset of frames and cells.

3.2. Implementation details

Image intensities are normalized to the interval $[0, 1]$ first. Then, images are background corrected by subtracting the smoothed image (large Gaussian kernel with σ_{bgr}) from the original image. Region histograms for computing the data costs in Equ. 1, are obtained from manual foreground and background scribbles drawn by the authors in one frame of each sequence (that is not contained in the segmentation ground truth). For graph construction we use an 8-neighborhood. The min-cut (with parameters λ, σ) is computed using the maxflow algorithm MATLAB interface [9]. Small segments below pixel area a_{min} are discarded. The method starts with segmenting the first frame and then segments subsequent frames using segmentation propagation. Erosion for foreground propagation is computed using a disk-shaped structuring element with radius s_{erosion}. For evaluation, segmentation masks are post processed by a hole-filling algorithm. We set these parameters: $\sigma_{\text{bgr}} = 20$px, $a_{\text{min}} = 500$px, $s_{\text{erosion}} = 15$px. Best performing parameters λ and σ were found by grid-search. The method was implemented in MATLAB.

3.3. Evaluation

Boundary detection results We compared the segmentation results obtained when using symmetric and asymmetric boundary costs in terms of boundary detection recall and precision. Recall measures the ratio of ground truth boundary pixels recalled by the computed boundary pixels within 4 pixels tolerance. We used the benchmark code from the Berkeley segmentation benchmark [10] to compute boundary detection results. Tab. 1 shows boundary detection results for both sequences and compares symmetric and asymmetric costs. The results show that asymmetric boundary costs perform better, especially in terms of recall. We also compared the stability of results when varying the min-cut parameters λ and σ. Fig. 4 shows that using asymmetric costs also yields more stable results.

Boundary costs	**Seq. 1** F-meas.	Recall	Prec.	**Seq. 2** F-meas.	Recall	Prec.
Symm.	0.863	0.838	0.889	0.768	0.732	0.808
Asymm. (Equ. 2)	**0.896**	**0.894**	**0.897**	**0.835**	**0.822**	**0.847**

Table 1: Boundary detection results on the PhC-C2DH-U373 *training* dataset with 4 pixels tolerance. For comparing symmetric and asymmetric boundary costs, best performing parameters λ and σ (in terms of F-measure) have been chosen for each setting. Parameters were obtained by grid-search over the parameter space, shown in Fig. 4.

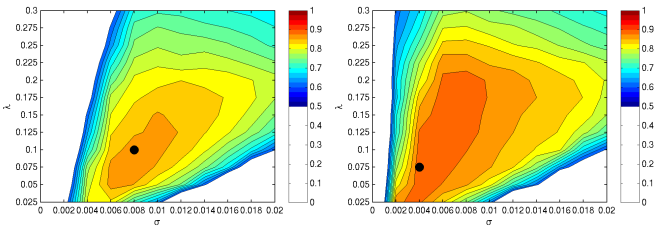

(a) Seq. 1 (symm.) (b) Seq. 1 (asymm.)

Fig. 4: Stability of results. F-measure of the boundary detection results as function of the parameters λ and σ. F-measure isolines are plotted in the range $[0.5, 1.0]$ in 0.025 intervals. Black dots indicate best performing parameters. **(a)** Results for the standard graph cut with symmetric boundary costs. **(b)** Results for our approach using asymmetric boundary costs. Our approach yields better results and is less sensitive to the selected parameters. Compare to Tab. 1.

Qualitative results In Fig. 5 qualitative segmentation results are given. They show improvements for detecting very weak phase contrast boundaries, e.g. Fig. 5a right column. Also the characteristic halo artifacts in phase contrast microscopy are handled well, due to segmentation at the correct dark-bright intensity transition. In contrast, symmetric boundary costs are strongly affected by the halo effect and predominantly show leaking segmentation at these borders.

Comparison to reported results We further evaluated our method using asymmetric costs in the measures of the ISBI Cell Tracking Challenge (CTC) [6]. The "average segmentation performance" (Av. SEG) measures the average intersection over union of all reference objects to their matching segmented objects. The "average tracking performance" (Av. TRA) measures how difficult it is to change the computed tracking graph to the ground truth graph. For more details, we refer to [6]. Tab. 2a summarizes our results for segmentation and tracking. For comparison Tab. 2b shows results of the top ranked methods reported at the Second CTC [6]. Although we could not perform a direct comparison on the *challenge* dataset yet[1], our results on the *training* dataset indicate a very competitive performance, especially for segmentation.

Sequence	Av. SEG	Av. TRA
Seq. 1	**0.8648**	0.9830
Seq. 2	**0.7563**	0.9150
Seq. 1+2	**0.8105**	0.9490

(a) Our results

Group	Av. SEG	Av. TRA
KTH-SE [3]	**0.7953**	0.9818
HOUS-US	**0.5323**	0.9206
IMCB-SG	**0.2669**	0.9595

(b) Reported results

Table 2: Results on the PhC-C2DH-U373 dataset in terms of the average segmentation and average tracking performance. **(a)** Our results on the *training* dataset, obtained using best parameters from grid-search ($\lambda = 0.2$, $\sigma = 0.006$), for best average segmentation performance on Seq. 1+2. **(b)** Results of top ranked methods on the *challenge* dataset, reported at the Second ISBI Cell Tracking Challenge [6].

Tab. 3 shows the gain achieved by adding segmentation propagation components for temporal consistency to our pure single-frame segmentation approach.

[1] Final ranking of the Third CTC is scheduled for May-June, 2015.

Segmentation propagation components	Seq. 1+2 Av. SEG	Av. TRA
Asymm. only	**0.7379**	0.8962
Asymm. + FP	**0.8027**	0.9370
Asymm. + FP + NM	**0.8105**	0.9490

Table 3: Segmentation propagation components. **Foreground propagation** (FP) yields significant improvements, since it supports the data costs in case of insufficient foreground evidence. The **non-merging constraint** (NM) improves results in case of false merging segments.

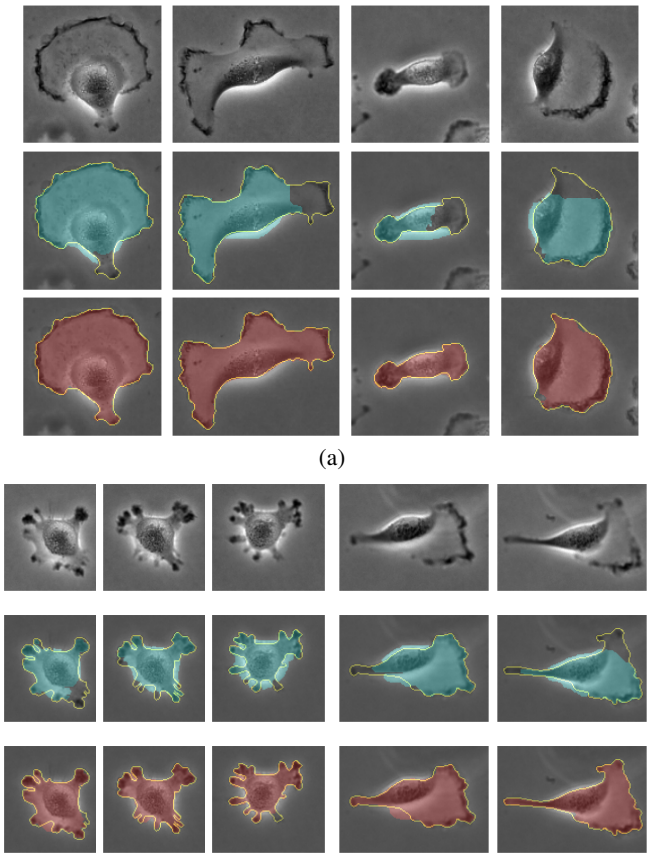

(a)

(b)

Fig. 5: Qualitative segmentation results. **Top rows** show the raw data. **Cyan masks** show results of the standard graph cut with symmetric boundary costs. **Red masks** show results of our approach with asymmetric costs. The ground truth contour is shown in yellow. **(a)** Single frame results for cells of Seq. 1. **(b)** Time lapse results of Seq. 2 for one cell on frames 5, 9, 15, and another cell on frames 62, 68.

4. CONCLUSIONS

The segmentation of cells in phase contrast images is significantly improved by using direction dependent boundary costs. Our approach outperforms the standard min-cut segmentation with symmetric boundary costs, and the top-ranked methods on the ISBI Cell Tracking Challenge 2014 dataset.

We assume that cell segmentation in other modalities (transmitted light, dark field, fluorescence, etc.) also profits from asymmetric boundary costs. Our open-source ImageJ plugin and the MATLAB implementation will enable a large audience to try it on their data sets.

5. ACKNOWLEDGEMENTS

We thank T. Brox for comments on the manuscript. This work was supported by the Excellence Initiative of the German Federal and State Governments (EXC 294).

6. REFERENCES

[1] F. Zernike, "Phase contrast, a new method for the microscopic observation of transparent objects part {II}," *Physica*, vol. 9, no. 10, pp. 974 – 986, 1942.

[2] D. Murphy, "Phase contrast microscopy," *Fundamentals of Light Microscopy and Electronic Imaging*, pp. 97–112, 2001.

[3] K. Magnusson, J. Jaldén, and H. M. Blau, *Cell tracking using bandpass filtering and the viterbi algorithm*, Description of the algorithm available at: http://www.codesolorzano.com/celltrackingchallenge/Cell_Tracking_Challenge/KTH-SE_files/isbi170.pdf.

[4] K. Li and T. Kanade, "Nonnegative mixed-norm preconditioning for microscopy image segmentation," in *Proceedings of the 21st International Conference on Information Processing in Medical Imaging*, 2009, IPMI '09, pp. 362–373.

[5] M.E. Ambül, C. Brepsant, J.-J. Meister, A.B. Verkhovsky, and I.F. Sbalzarini, "High-resolution cell outline segmentation and tracking from phase-contrast microscopy images," *Journal of Microscopy*, vol. 245, no. 2, pp. 161–170, 2012.

[6] *ISBI Cell Tracking Challenge*, Available at: http://www.codesolorzano.com/celltrackingchallenge.

[7] Y. Boykov and G. Funka-Lea, "Graph cuts and efficient n-d image segmentation," *International Journal of Computer Vision*, vol. 70, no. 2, pp. 109–131, 2006.

[8] M. Maška, V. Ulman, D. Svoboda, P. Matula, and P. Matula, *et al.*, "A benchmark for comparison of cell tracking algorithms," *Bioinformatics*, vol. 30, no. 11, pp. 1609–1617, 2014.

[9] Y. Boykov and V. Kolmogorov, "An experimental comparison of min-cut/max- flow algorithms for energy minimization in vision," *Pattern Analysis and Machine Intelligence, IEEE Transactions on*, vol. 26, no. 9, pp. 1124–1137, Sept 2004.

[10] *The Berkeley Segmentation Dataset and Benchmark*, Available at: http://www.eecs.berkeley.edu/Research/Projects/CS/vision/bsds/.